University of Windsor

Scholarship at UWindsor

2010

Single frame super-resolution image system

Fei Yu
University of Windsor

Single Frame Super-Resolution Image System

by

Fei Yu

A Thesis
Submitted to the Faculty of Graduate Studies
through Electrical Engineering
in Partial Fulfillment of the Requirements for
the Degree of Master of Applied Science at the
University of Windsor

Windsor, Ontario, Canada

2010

AUTHOR'S DECLARATION OF ORIGINALITY

I hereby certify that I am the sole author of this thesis and that no part of this thesis has been published or submitted for publication.

I certify that, to the best of my knowledge, my thesis does not infringe upon anyone's copyright nor violate any proprietary rights and that any ideas, techniques, quotations, or any other material from the work of other people included in my thesis, published or otherwise, are fully acknowledged in accordance with the standard referencing practices. Furthermore, to the extent that I have included copyrighted material that surpasses the bounds of fair dealing within the meaning of the Canada Copyright Act, I certify that I have obtained a written permission from the copyright owner(s) to include such material(s) in my thesis and have included copies of such copyright clearances to my appendix.

I declare that this is a true copy of my thesis, including any final revisions, as approved by my thesis committee and the Graduate Studies office, and that this thesis has not been submitted for a higher degree to any other University or Institution.

ABSTRACT

The estimation of some unknown quantity information from known observable information can be viewed as a specific statistical process which needs an extra source of information prediction strategy. In this regard, image super-resolution is an important application.

In this thesis, we proposed a new image interpolation method based on Redundant Discrete Wavelet Transform (RDWT) and self-adaptive processes in which edge direction details are considered to solve single-frame image super-resolution task. Information about sharp variations, both in horizontal and vertical directions derived from wavelet transform sub-bands are considered, followed by detection and modification of the aliasing part in the preliminary output in order to increase the visual effect. By exploiting fundamental properties of images such as property of edge direction, different parts of the source image are considered separately in order to predict the vertical and horizontal details accurately, helping to consummate the whole framework in reconstructing the high-resolution image.

Extensive tests of the proposed method show that both objective quality (PSNR) and subjective quality are obviously improved compared to several other state-of-the-art methods. And this work also leaved capacious space for further research, not only theoretical but also practical. Some of the related research applications based on this algorithm strategy are also briefly introduced.

DEDICATION

To my beloved mother.

ACKNOWLEDGEMENTS

There are several people who deserve my sincere gratitude for their great help.

First and foremost, I would like to give my sincere gratitude to my supervisor Dr. Jonathan Wu for all of his generous support and guidance. His advice and irreplaceable help, both academically and personally, have had, and will continue to have, a tremendous impact on my life.

Faculty at the University of Windsor, including my committee members Dr. Mohammed A. S. Khalid and Dr. Dan Wu from school of computer science are also those I am very grateful to.

Also, I want to thank Ms. Andria Ballo (nee Turner) for her irreplaceable assistance and cheerful conversation with me.

Moreover, I would like to offer great gratitude to Dr. Guanghui Wang and Mr. Michael Chukwu for their sound technical advice and kind sharing of their opinions.

Finally, I must extend my most sincere love and gratitude to my parents, especially to my mother for her abiding support and enthusiasm.

Table of Contents

LIST OF FIGURES

LIST OF TABLES

LIST OF ABBREVIATIONS

SR: Super Resolution

HR: High Resolution

LR: Low Resolution

PSNR: Peak Signal to Noise Ratio

RDWT: Redundant Discrete Wavelet Transform

DWT: Discrete Wavelet Transform

IDWT: Inverse Discrete Wavelet Transform

PCA: Principal Component Analysis

HMT: Hidden Markov Tree

MLP: Multilayer Perception

CDF: Cohen-Daubechies-Feauveau

MSE: Mean Square Error

dB: decibel units

HD: High Definition

CHAPTER 1

INTRODUCTION

1.1   Problem Statement

As one of the most important information carriers in modern life, images have irreplaceable positions in many areas. With the development of modern image processing technology and increasing computational power, we can overview many classic algorithms from a time-consuming point of view. Among them, pursuing high-resolution (HR) or Super-resolution (SR) images is always a difficult, though very important task. The requirements of HR exists not only in daily life (i.e. entertainment, surveillance, media, medical area), but also in national defense, remote sensing and communication, and so many other areas.

Normally, we can choose hardware artifices to fulfill this task by reducing the pixel size when manufacturing optical instruments. However, it is well known that there exists optical limitations within unit pixel size, and ignoring that will engender shot noise and exponentially increase the device price. Thus, people try to solve this problem from a software point of view. Being more specific, from a signal processing point of view, image resolution up-conversion is a process focusing on the up-sampling of the already digitally sampled signal; while from an image processing point of view, increasing the resolution of an image is a process which generates or recovers a higher resolution image from one or more low resolution image resources. Both sides present a significant challenge because of the uncertainty of the original source.

Single-frame input and multi-frame input are two situations we face when trying to pursue SR images. A multi-frame input means a series of input images (or a part of a

video) which have different sub-pixel shifts, and each of them contain highly-related information (i.e. relative scene motions) which can be exploited to obtain a SR image [1]. However, most of the time, we do not have enough related input image sources at hand. This requires us to develop the algorithm based on single-frame input SR, meaning the input source is a single raster image. In other words, the single-frame SR is also known as image scaling, interpolation, zooming and enlargement [2]. The requirement of solving such a single frame image super-resolution problem arises in several practical situations [5]. In investigative criminology for example, we always face the problem that one has available face and fingerprint databases but only a single observation for the suspect. That specific given low resolution (LR) image may be used to generate the very HR image we need with no other related information provided. Similarly, a situation can be found when a particular LR text image is enhanced to generate HR images. We can see an example of single frame image resolution enhancement from Figure 1.
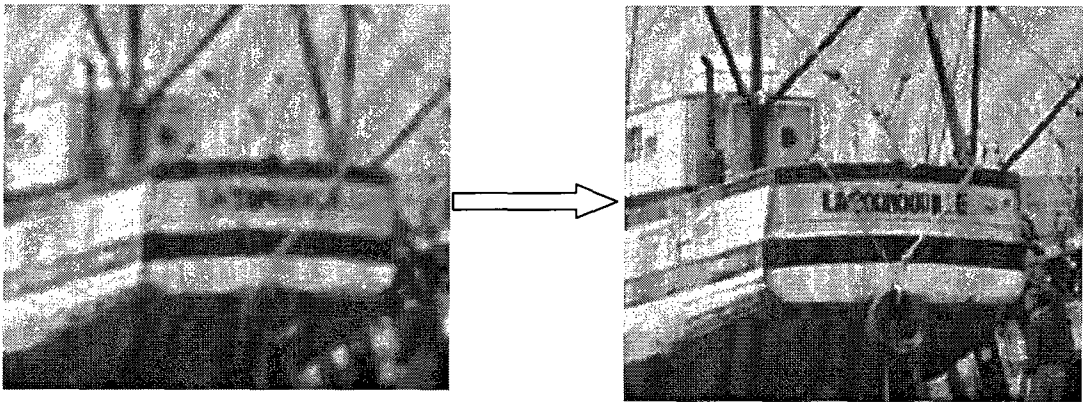
Resolution = 64 x 64   Resolution = 256 x 256

Figure 1 Single-frame image resolution enhancement example

(resolution 64 x 64→256 x 256)

1.2 Thesis Highlights and Contributions

This thesis presents a general investigation on the main classification of single-frame image super-resolution algorithms and proposes a novel proposed SR algorithm based on the combination of redundant discrete wavelet transform (RDWT), edge-adaptive and aliasing removal strategies. Lots of input images are used in the proposed design to assure the robustness of the algorithm. And by using the proposed system, we try to solve the main challenges in traditional SR problems, which are to find a way to de-blur, de-noise and de-alias way so as to increase spatial resolution.

The principle advantage of this scheme lies in its high efficiency and stability in various kinds of images. The outputs show obvious improvement on the performance of the existing techniques. Though the proposed algorithm is derived from the ideas of some core functionalities found in some existing research, the improvement of the whole system constrains the feasible solutions for the prediction of the unknown coefficients.

In addition, since the whole system is modularized and every part can be substituted by more flexible or more advanced algorithms, there will be plenty of spaces left for modification in order to extend the capability. Some of the potential changes will be discussed later in this thesis as well, so that those who are interested will have the benefit of this research.

1.3 Thesis Organization

The thesis begins with a general overview of the image super-resolution conception and classification followed by the motivation and challenges in the single-frame super-resolution mission. Contributions and brief discussions of this work are also provided.

Chapter 2 gives a review of the history of the development of super-resolution methods. State-of-art literature is reviewed in order to follow the classification of the strategy used in each work.

Chapter 3 is focused on the introduction of the main principal of all conceptions which are used in the proposed algorithms. We explain edge modeling, wavelet-based interpolation, aliasing detection and rectification using mathematical methods and other image processing techniques.

Chapter 4 initially introduces the details about the proposed single-frame SR algorithm, following the order of the whole system, which can be divided into parts like preprocessing, super-resolution and analysis, and the detection and correction of the potential aliasing areas. At the same time, some of the related applications are briefly introduced; for example, image changing detection and foreground extraction, including the principle and the flows of the proposed algorithms are examined.

Chapter 5 shows the standard which is used to judge the SR algorithms and the detailed experimental data of the experiment on the proposed algorithm. Then the experimental results for the real images are shown followed by the analysis of the result and the comparison of the outputs between the proposed algorithm and the state-of-art literature. Also, the outputs of the related algorithms such as image foreground extraction and changing detection are shown as well.

Chapter 6 gives a summary of contributions and conclusions presented in this work, followed by a prospect for future work.

CHAPTER 2

REVIEW OF STATE-OF-ART LITERATURES

2.1 Overview of SR Algorithms

As the importance of SR in the image processing area is so obvious, there are lots of SR methods and surveys on those methods in research literature. Among them, many significant surveys [2] [3] [4] [5] [6] can be used to start with our study in this classical area. Though they all have their own points of emphasis on different kinds of algorithms, the main clue they try to exploit is the strategy to solve the specific tasks in SR reconstruction techniques which are de-blurring, de-noising, and alias removal, and the comparison of the effects from the experiment outputs.

In general, the SR algorithms can be divided into two groups: reconstruction-based and learning-based [5]. When we mention reconstruction-based SR, in most cases, we have to find a way to recover a HR image from several LR observations. To do this some cues are always needed, in order to find the relationship between those LR inputs. Based on motion cues much existing literature examines sub-pixel shifts among the different LR images in order to find a clue with which to interpolate them onto a HR grid. This is followed by restoration to remove blur and noise. According to [1], there are multiple studies from both time domain and frequency approaches. As for learning-based SR algorithms, a database of several other similar images is needed in order to find a prior on the original HR image. Among them, neural network is a good instrument for users to find a stable relationship between each input [1]. However, as these methods always require multiple inputs, we will discuss more about single-input algorithms in the following parts.

As for still image SR algorithms, we classify them into global and local items [5]. There is a model of the relationship between a HR image and single-input image as shown in Figure 2.
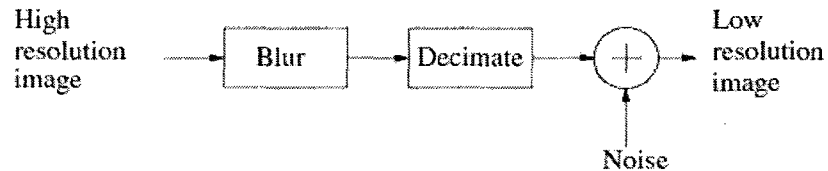
Figure 2 Relationship between HR and single LR

Illuminated by [8], the Papoulis–Gerchberg method [7] is an example of global approaches in which the input LR image is considered to be a single entity for processing. The main idea is that if the measurements of the object spectrum are nearly noise free, then the entire spectrum of the object can be generated uniquely using the principle of analytic continuation. This is a good idea in both single and multiple input situations; however, the result cannot be controlled well if the noise is obvious. Principal component analysis (PCA) –based global learning method for super-resolution reconstruction [4] [9] is a global learning method, which tries to obtain a few significant eigenimages of a database of several similar HR images. The characteristic of these eigenimages are then be used to compute the coefficients needed for up-sampling the LR image. However, this kind of method suffers from the infection of the blur existing in the input. Consequently, the associated eigen expansion between blur LR image and the related HR database will be very poor in producing the ideal HR image. And the detail of the image, for example edge, is independent within the database and is hard to spread follow the eigen expansion.

Local SR approaches are good choices for the consideration of edge details. We can start from Kernel SR algorithms which are amply discussed in [2]. A basic function is needed to approximate the continuous function needed to underlying the discrete samples that make up the HR image. As is well known to all, linear and cubic kernels can be used which are the basic idea of bilinear and bicubic interpolations. Those are widely used for

the convenient of kernel calculation. The idea in [10] is a method trying to divide the pixels into classes like flat and edge areas, and then treat them separately when doing the enlargement. The idea of adding weight from different direction of the details is a good start. [12] is similar to this because each pixel belongs to a single class instead of multiple classes. Neural network can be used in local method as well [11]. Pixels consists of the around the source pixel in the local window are used as the input for the neural network, and the neural network can be trained by using a decimated image as input and the corresponding original image as target in order to get the output consists of the pixels needed for the super-resolved image. Sparse derivative is used in [13] which attempts to use the distribution of the derivative of natural images as a model to exploit SR image. One of the advantages of using local approaches is that the edge information can be properly reserved. When dealing with a noisy source, it is necessary to present a smart interpolation way by anisotropic diffusion in order to sharpen edges and generate plausible detail [14] [15]. This strategy may show a smooth effect around the edge area, however, distortion is unavoidable. Xin Li produced similar work in [16] called new edge-directed interpolation, by using the duality between the low resolution and high resolution covariance for SR processing. He found a clue between the covariance of neighboring pixels in local windows around the LR source and those in the HR target. Direction of diagonal neighbors are considered in the first pass, followed by the second pass, which uses horizontal and vertical neighbors to interpolate the rest of the pixels. In [17] we can find a locally-adaptive zooming algorithm which is set point on discontinuities and sharp luminance variations while doubling the LR source in horizontal and vertical directions. All of them make good use of local edge information to predict the detailed local areas in the output HR image. This is a great direction of research to be continued.

2.2 Wavelet-Based SR Algorithms

Wavelet-based SR algorithms are unique and irreplaceable contributions in all kinds of SR algorithms, and we can find the discussions about the merits and pitfalls of different kinds of wavelet-based SR algorithms in almost all good surveys in SR area; for example in [1]-[6] [18] [19]. Analysis LR from a wavelet point of view gives us a better understanding of the possibility of increasing the resolution of signal and the possibility of using all kinds of wavelet instruments which have proved to be good at forecasting tasks; instead of simply using traditional image enhancement strategies. Multi-resolution analysis of the input signal is widely used and has proved to be powerful in wavelet-based SR areas because the signal structure similarity across the scales of the decomposed LR source can be found to predict the next higher fine scale of detail coefficients. However, there are divergences of approach occurring in the method of prediction.

Hidden Markov Tree (HMT) has been widely used in wavelet processing areas. [20] sets up a method using HMT to predict the next set of coefficients using training data. This has shown better HR results than traditional interpolation algorithms such as bilinear ones. [21] follows the same clue but makes some additional modifications by eliminating the requirement for training and simplifying the coefficient sign prediction method. These two methods are computationally efficient, and the quad-tree they propagated is the magnitude the parents coefficients to the child level, which yields unpredictable results.

Neural network can be well used in wavelet SR as well [23]. Multilayer perception (MLP) interpolation schemes based on the wavelet transformation and sub-band filtering are proposed [23]. The sub LR image signal can be viewed separately, and then the MLP progress is used to predict the corresponding coefficients needed in the related HR image. As the wavelet analysis/synthesis procedure and MLP procedure can be implemented easily by using VLSI techniques, this kind of methods can be implemented on hardware as well. However, the veracity of the output is fair, and the system is not that stable and may yield distortion if the source is not well selected.

Like traditional SR algorithms, local details such as edge information are still a very important direction which has been extensively studied and used. Directional wavelet filtering has been used in [22] to ensure the effect of the output in the direction of the detail edges. Multiple and flexible directional filtering is used to model the characteristics of the target image edges. Though performing well on complex LR images, [22] provides marginal gains in less complex ones. Markov Chain Monte Carlo is widely used in wavelet analysis and has also been used in [24] to synthesize a system which is edgily adaptive.

There is a special family of wavelet-transform modulus which tries to maximize capturing the sharp variation points of signals. Then it tries to follow the local Lipschitz regularity across the scales, which characterizes [25] [26] [27]. This is one of the most important instruments we use in our proposed algorithms, and we will specifically discuss this later. Grace et al. attempt to extend this work into the single-frame image SR area by [28], and then they consolidate their work in [29]. From a spatial point of view, they proposed an algorithm which uses wavelets to extract sharp variations in the LR image and use this information to adapt to the image to local singularity characteristics. This strategy, though suffering from high complexity, yields sharper images in the output. Edge information, which is very important in SR area, is well protected to a great extent. The visual quality of the output images is not sensitive to the accuracy of the model, making the whole system robust. However, aliasing still seems to be a key problem they face judging from the visual effect.

Another class of local approaches we would like to supplement here is SR through the local linear embedding in contourlet domain. It is similar to wavelet-based SR algorithms; and also, it is further capable of capturing the smoothness along contours making use of directional decompositions [5] [30] [31]. A set of high resolutions have been trained locally in order to get the information we need to predict the contourlet coefficients at the finer scales of the unknown high resolution image. The inverse contourlet transform

action is performed later using the learnt coefficients which recover the super-resolved image. In effect, we can tell from the output of their experiment that edge information can be well protected by using the high resolution representation of an oriented edge primitive from the training data, while the use of wavelets alone can only allow us to capture horizontal and vertical edges properly. Normally, because the training set may have different average brightness values, the contourlet coefficients in all subbands, except at the lowpass subband where we obtain the contourlet coefficients, should be acquired from a suitably interpolated version of the LR image [32]. This will cause a time consuming burden and cannot avoid the transference of the aliasing effect as well.

On the whole, all these unique works we introduced here suffer from several drawbacks from some perspectives, yet provided great and promising paths and ideas for us to explore for our proposed system.

CHAPTER 3

ANALYSIS OF WAVELET-BASED SR ALGORITHM

3.1   Wavelet Domain Edge Analysis

Edge can be described as a form of information in the spatial domain and wavelet domain, which is used to do image processing or signal processing. It is helpful in the whole image modeling process, as well as in handling detailed parts of the images, where the most important information may be found. By studying the changes in the neighborhood of the edges, it may be possible to find a useful changing disciplinarian which can used to predict whole images or entire singles.

Starting with a brief overview of edge performance in the spatial domain will give us a clear understanding of the changes they cause in continuous space. There are two key observations we focus on: a sharp transition of the image intensity, which happens across the edge orientation and the image intensity field, which is almost uniform when we follow the same side of the edge orientation [33]. With these properties, we can easily track the changes of the information when we digitize the image intensity field into data arrays. By checking the example in Figure 3 [33] below, there is a clearer sense about what we are trying to explain here. It is obvious that the local gradient and the rate of change in itself when doing down-sampling is where we should keep our emphasis on.
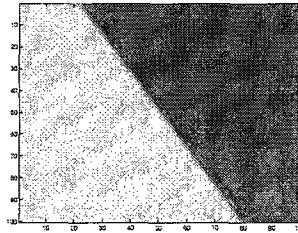
Figure 3 Digitized image containing edge information

A similar situation happens in the wavelet domain as well. By using decimated wavelet transforms with equal decimation rationing along the horizontal, vertical, and diagonal directions, we can trace the geometric constraint as we explained in the spatial domain, not to mention if a linear non-decimated wavelet is used. By tracing the changes of the wavelet transform along different levels, and due to the frequency aliasing introduced by the decimation, the edge information can be easily located.

To extend the work in [25] [26] [27], which tries to maximize capturing the sharp variation points of signals, and then tries to follow the local Lipschitz regularity across the scales characterizes what we mentioned in the last chapter where we explained the wavelet framework as follows [29].

In multi-scale wavelet domain, we normally trace information along scale "s" to determine the global or local nature of the signal features. At the scale "s", the wavelet transform of a signal $W_s f(x)$, which is defined as the following function (1), can be viewed as the first derivative of $f * \theta_s$, while an extremum of small magnitude indicates a region of relatively slow variation. It is useful to locate the sharp transition regions.

$$W_s f(x) = f(x) * \left(s \frac{d\theta_s(x)}{dx} \right) = s \frac{d}{dx} (f * \theta_s)(x)$$ (1)

where $\theta_s(x) = \frac{1}{s}\theta\left(\frac{x}{s}\right)$ is a smooth function integrates to 1 and converges to zero at infinity.

To further explain and make it more common, if θ_s is Gaussian, the detection of local extrema corresponds to the well known Canny edge detector [34].

Extending (1) into two dimensions, we have $W_s^1 f(x,y)$ and $W_s^2 f(x,y)$ for the wavelet transform of $f(x)$, we have the local maximum at the greatest gradient as shown in equation (2), which indicates the edge information locally.

$$W_s f(x,y) = \sqrt{\left|W_s^1 f(x,y)\right|^2 + \left|W_s^2 f(x,y)\right|^2}$$ (2)

12

3.2   Wavelet Based Interpolation

3.2.1. Discrete Wavelet Transform (DWT)

The defined problem within the context of wavelet inspired techniques is modeled after the prediction of the unavailable higher detail wavelet coefficients. The discrete wavelet transformation is well proven to be a good way to deal with interpolation problem which uses low-pass and high-pass filters, $h(n)$ and $g(n)$, to expand a digital signal. They are referred to as analysis filters. After DWT, the coefficients c_k (coarse coefficients) and d_k (detail coefficients) are produced by convolving the digital signal with each filter and then decimating the output. Coarse coefficients provide information about low frequencies, while detail coefficients provide information about high frequencies. Most existing DWT-based algorithms focus on predicting the needed high coefficients in order to synthesize the high-resolution image.

3.2.2. Redundant Discrete Wavelet Transform (RDWT)

To generate a k-times larger size image than the original image with maximum image details such as edges, corners etc. are the fundamental concept of the image interpolation. As mentioned, we focus on generating a noise-free, blur-free, and alias-free interpolation algorithm, which means we need as much input information as possible to solve this ill-posed problem.

The use of decimators makes the DWT more computationally efficient by ignoring redundant coefficients. However, these coefficients may be potentially very valuable information needed in the reconstruction process (reducing aliasing, etc.). For the consideration of this it is beneficial to remove the decimators. That is why we use RDWT in this proposed algorithm, and the process of RDWT is shown in Figure 1 where the original image can be divided into the approximation part, the horizontal details, the vertical details and the diagonal details. In the decomposition structure of the 2-D RDWT, Ω_{jm} is the m-th sub-sapce on the j-th level, $S_{i,k}(\Omega_{jm})$ is a circulant shift of Ω_{jm} with a i-step shift on x-direction and a k-step shift on y-direction. Also, we can find in Figure 2, which

is an example of the RDWT shown in Figure 1, a 512×512 image will generate one 512×512 coarse sub-image and three 512×512 detail ones after RDWT, which is 1024×1024 values, that is obviously much more than 512×512 after DWT.

$$\Omega_m^j$$

$$DWT(S_{0,0}(\Omega_m^j)) \qquad DWT(S_{1,0}(\Omega_m^j)) \qquad DWT(S_{0,1}(\Omega_m^j)) \qquad DWT(S_{1,1}(\Omega_m^j))$$

$$\Omega_{4m}^{j+1}\Omega_{4m+1}^{j+1}\Omega_{4m+2}^{j+1}\Omega_{4m+3}^{j+1} \qquad \Omega_{4m+4}^{j+1}\cdots\Omega_{4m+7}^{j+1} \qquad \Omega_{4m+8}^{j+1}\cdots\Omega_{4m+11}^{j+1} \qquad \Omega_{4m+12}^{j+1}\cdots\Omega_{4m+15}^{j+1}$$

$$\Omega_{16m}^{j+2}\Omega_{16m+1}^{j+2}\cdots\Omega_{16m+15}^{j+2} \qquad \Omega_{16m+16}^{j+2}\cdots\Omega_{16m+31}^{j+2} \qquad \cdots \qquad \Omega_{16m+48}^{j+2}\cdots\Omega_{16m+63}^{j+2}$$
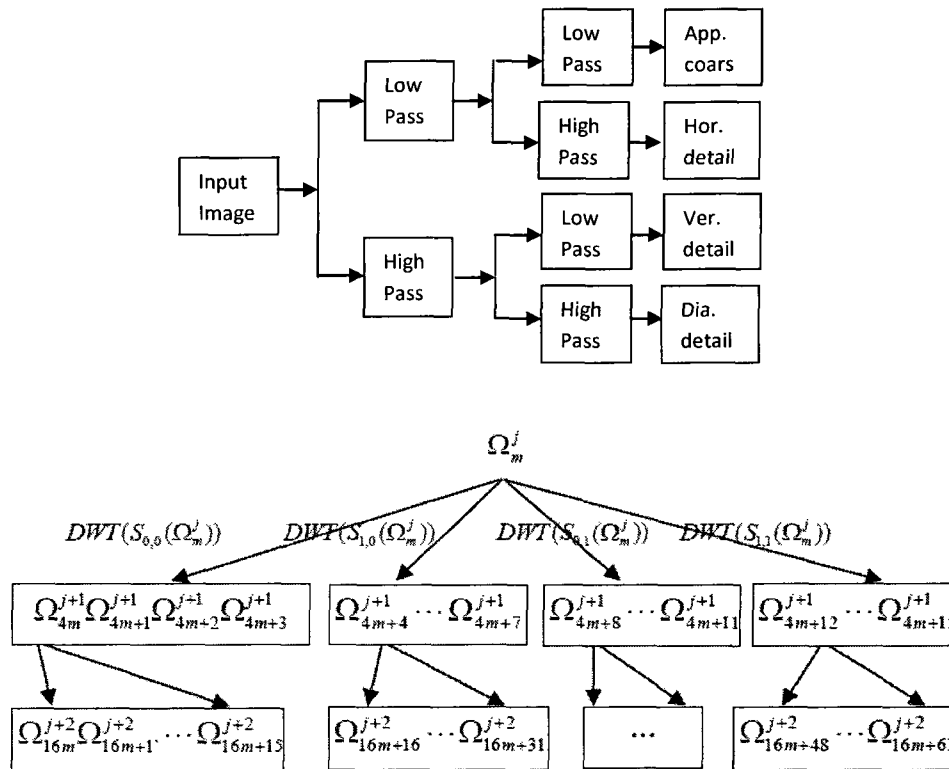
Figure 4 Redundant DWT decomposition of image
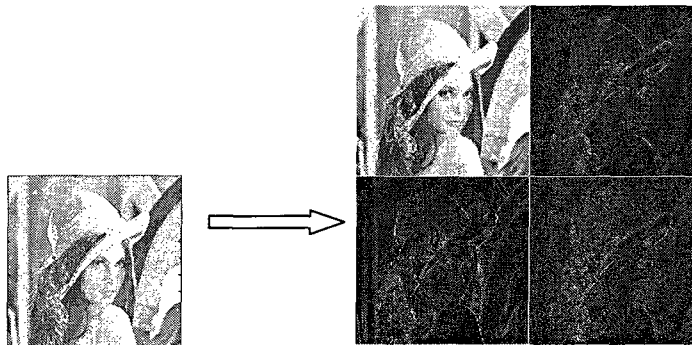
Figure 5 Redundant DWT decomposition of Lena (512×512→1024×1024)

3.2.3. Inverse Discrete Wavelet Transform (IDWT)

In order to do interpolation, which is up-sampling in the wavelet domain in a sense, we have to know the detailed information in vertical, horizontal, and diagonal directions. Furthermore, we have to do an inverse calculation of the process shown in Figure 4 and 5 (up sample process needed after each filter), which means we need the information about the one coarse part and three detailed parts of the target image. The prediction of the detailed information section is explained in the following chapters as implementation details. As long as we have all the information we want, IDWT will be done to get the HR image we need. Figure 6 is a sketch map on Lena for IDWT. It is sample produced by deciding where original size 512×512 image will be enlarged to size 1024×1024. Theoretically, any size of interpolation can be achieved by using this strategy.
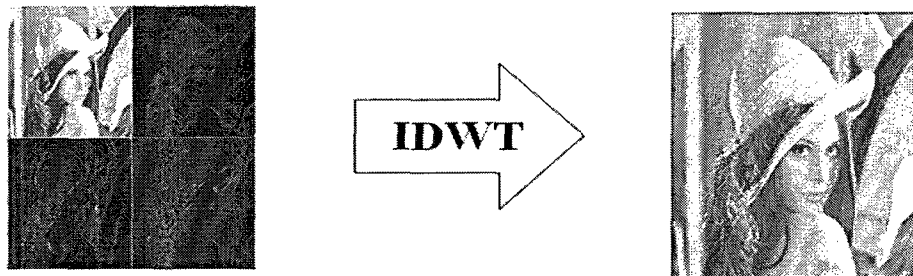
Figure 6 IDWT sketch of Lena (4×512×512→1024×1024)

3.3 Aliasing Areas Analysis

As defined in digital processing area, in signal processing and related disciplines, aliasing refers to an effect that causes different signals to become indistinguishable from each other (or aliases of one another) when sampled. It also refers to the distortion or artifact those results when the signal reconstructed from samples is different than the original continuous signal. Functions whose frequency content is bounded (band limited) have infinite duration. If it is sampled at a high enough rate, as determined by the bandwidth,

the original function can be perfectly reconstructed from the infinite set of samples in theory. Figure 7 is a sample of non-aliasing and aliasing situation.
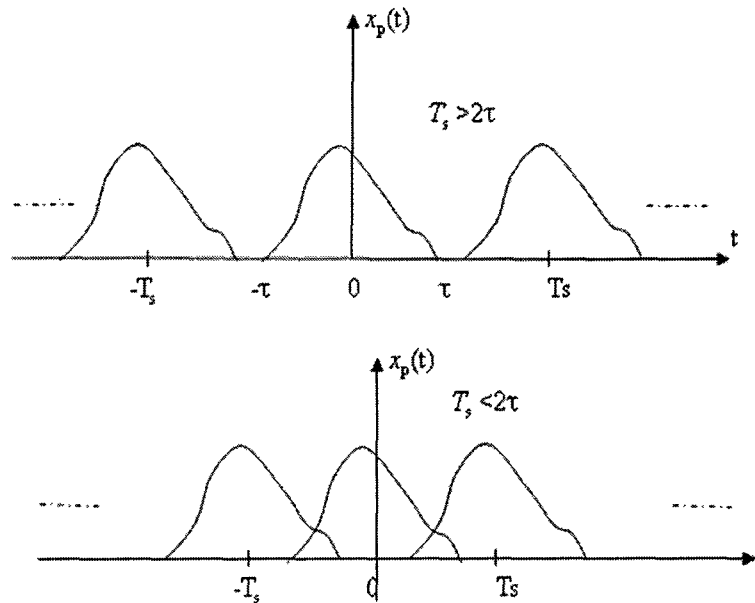
Figure 7 Sample of aliasing

As in the SR area, original images can be viewed as an already down-sampled single which will undoubtedly contain areas of aliasing. Those areas will provide distortion which completely erodes the inter-scale dependency of the coefficients. If this phenomenon is ignored, the effect will pass along on the aliased image pixels resulting in the degeneration of the estimated higher resolution outputs. Figure 8 is an example using the image Barbara as input. We can find significant aliasing along the headband of the woman on the right image compared to the original one on the left. Therefore, we need a method to efficiently extract the aliasing areas of the original image and handle those separately. Since aliasing may have reaction in both the time and frequency domains, it can be analysis separately to increase the accuracy.

Figure 8 Sample of aliasing using Barbara as input

In the frequency domain, high magnitude coefficients with a corresponding high decay rate will indicate an inadequate sampling rate and possible aliasing. This can be tested by tracing the wavelet changes along different scales while doing decompositions. While in the time domain, areas of the images with singularities and edges at the same rate as the image spatial resolution can be potential aliasing areas.

Though the potential aliasing areas are fairly complex to accurately estimate in a SR system, they do need to be accurately detected and properly and separately handled while doing predictions, before the IDWT, in order to increase the veracity of the output HR image.

CHAPTER 4

PROPOSED ALGORITHMS

4.1 Proposed Edge-Adaptive SR Algorithm

4.1.1 Preprocessing

As discussed by Nyquist & Shannon, we face an ill-posed question because if we define the HR image as the target signal. As we only have one low-resolution image as input, which is part of the original signal, it is not possible to recover the whole original signal (especially the detail high frequency parts already ignored). In order to fulfill the task which relies on a single input LR image to generate a HR output image, we decided to use the wavelet method mentioned before. Some ideas derive from the core functionalities of the existing methods we mentioned in the previous chapters; however, we focus on the definitive model that constrains the feasible solutions for the prediction of the coefficients.

To begin with, the input image is decomposed by RDWT, which is an over-complete representation of the coefficients at each scale. The benefit of using RDWT has been discussed before, giving us additional information for solving linear equations later. Moreover, by using RDWT one can obtain L DWT results by only decomposing an L-length signal x(k) and its one step shift, instead of decomposing each shift of x(k) respectively. Alternatively we can say that this redundancy provides flexibility and compatibility for more stability and robustness. [35].

The Cohen-Daubechies-Feauveau (CDF) 9/7 bi-orthogonal symmetric wavelets, which are well used in JEPG 2000 lossy compression, is used throughout the wavelet multi-resolution analysis and synthesis progress. CDF 9/7 share properties that all generators

and wavelets in this family are symmetric. This fact is used to ensure the robustness of the decomposition and reconstruction process. The detailed coefficients of the CDF 9/7 wavelet is given in Table 1 [36].

Table 1 CDF 9/7 Coefficients

k	Analysis lowpass filter $(1/2\ a_{dual})$	Analysis highpass filter (b_{dual})	Synthesis lowpass filter (a_{prim})	Synthesis highpass filter $(1/2\ b_{prim})$
-4	0.026748757411	0	0	0.026748757411
-3	-0.016864118443	0.091271763114	-0.091271763114	0.016864118443
-2	-0.078223266529	-0.057543526229	-0.057543526229	-0.078223266529
-1	0.266864118443	-0.591271763114	0.591271763114	-0.266864118443
0	0.602949018236	1.11508705	1.11508705	0.602949018236
1	0.266864118443	-0.591271763114	0.591271763114	-0.266864118443
2	-0.078223266529	-0.057543526229	-0.057543526229	-0.078223266529
3	-0.016864118443	0.091271763114	-0.091271763114	0.016864118443
4	0.026748757411	0	0	0.026748757411

In order to ensure the comparability of the results, we keep the source image as the original one, and down sample the image using CDF 9/7-based DWT to reduce that into half of the size. Then, the downsized image is used as the input image and decomposed into different scales (see Figure 9).
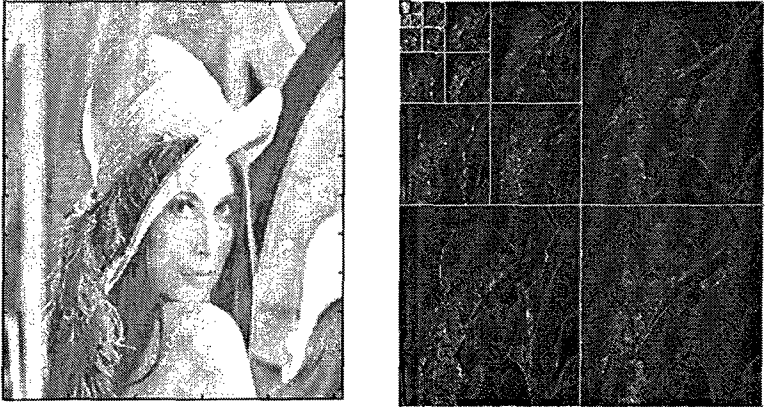

Figure 9 Decomposition of input image (using Lena as an example)

Information of different scales (s_0, s_1, s_2 ...) is saved separately according to the scale they belong to, and that information is classified into three sorts: horizontal, vertical, and diagonal. Since various kind of images have different information in different directions (e.g. horizontal details (Boats) and vertical details (Peppers)), and different weighting strategies can be realized within different sorts.

4.1.2 Super-resolution Realization

It is well known that feature information is always important in image processing. Finding sharp variations (e.g. we use the Canny edge detector to find a local maximum) is the way we can use to obtain edge information. Many previous studies, as previously discussed, show that a multi-scale edge characterization framework is a convenient analysis of edges in the wavelet domain which is used here as well. In this section and the next, we first present the mathematical process of the proposed edge-adaptive algorithm and then describe the process of IDWT.

Starting with wavelet multi-resolution approximation modeling, we may find that there is a conjunction function f, of which there is an orthogonal projection at the scale s (2^j) on space W_j. The approximation between two continuous scales s (2^j) and $s\text{-}1$ (2^{j-1}) are respectively equal to their projections on the two consecutive spaces, that is W_j and W_{j-1}. Moreover, we can find some relationship between these two spaces by the expression of the following equation 3.

$$W_{j-1} = W_j \oplus V_j \tag{3}$$

where V_j is the passing orthogonal factor of W_j in W_{j-1}. Hence, the projection function f can be the combination of projections on W_j and V_j. Furthermore, V_j contains the detailed information of the projection on the next space, i.e. V_{j-1}, which cannot be found in the source space V_j. Based on the wavelet decomposition analysis, we can trace this orthogonal projection of iteration through the following equation 4, and get the information we needed throughout the wavelet analysis.

$$W_j = W_{j+1} \oplus V_{j+1} \tag{4}$$

This makes the process like a regression which has some relationship linked by specific coefficients between each other, and it is our job to use some mathematics parameters to unfurl this relationship. The Lipschitz Exponent is the one we choose [26] [27].

In particular, for the convenience of computation on the singularity problem shown in equation 2 before, we introduce Lipschitz Exponent α. A function $f(x)$ is uniformly Lipschitz α over an interval (a,b) if and only if there exists a constant $K > 0$ such that for all $x \in (a,b)$, the wavelet transform satisfies equation 5 [28].

$$\left| W_s f(x) \right| \le K s^\alpha \tag{5}$$

In this case, if we assume the conjunction function f between the two continues space W_j and W_{j-1} is uniformly lipschitz, then the two projections, i.e. V_j and V_{j-1} are linearly related too, as shown in equation 6.

$$V_j \propto T \cdot V_{j-1} \tag{6}$$

As we focus on the local Lipschitz parameters of the difficult singularities, the task of estimating the details in scale 0 is equivalent to find K_m and α_m as shown in equation 7.

$$W_{2^j} f\left[x_m^{(j)} \right] = K_m \left(2^j \right)^{\alpha_m}, \qquad j=1,\dots,J \tag{7}$$

To recover K_m and α_m in equation 7, we only need to solve the following linear regression equation 8.

$$\log_2 \left(W_{2^j} f\left[x_m^{(j)} \right] \right) = \log_2 K_m + j\alpha_m, \ j=1,\dots,J \tag{8}$$

As long as we use RDWT in the preprocessing process, and have plenty of high-resolution classified information, we can obtain the Lipschitz parameters from the above equations, and the decay rate instead is considered. We then calculated the absolute maximum value of the coefficients. The slope of the $\log 2$ between the coefficient and the absolute value of the coefficient in the same position in the next higher scale is the Lipschitz exponent for these two adjacent scales (Figure 10 &11). By calculating the growth rate σ between each scale s in the vertical and horizontal details separately, and

21

assuming that s_1 and s_0 have the same coarse components, we have sufficient information for the reconstruction of the high-resolution image.
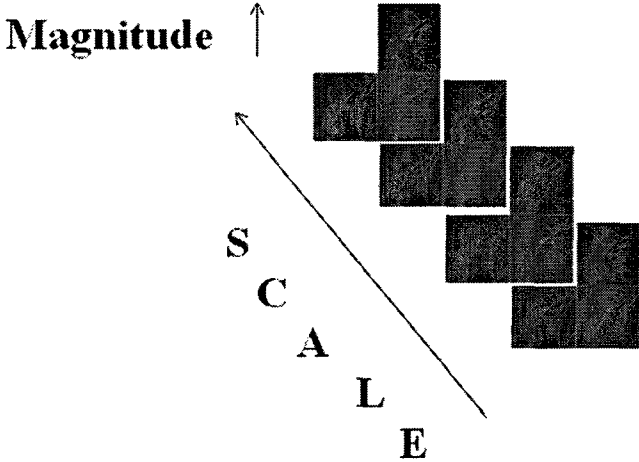

Figure 10 Scale and magnitude propagation analysis (using Lena as an example)

Figure 11 Horizontal growth rate propagation (other direction similar)

4.1.3 Aliasing Processing & Feature Constrain

As discussed before, we can detect the potential aliasing areas through both frequency and time domains, which jointly provide an excellent indication of aliasing in the original input image. In the time domain, the expression is a high pass operator dealing with the inter-pixel singularities and edges information, while in the frequency domain, we focus on those areas with high magnitudes as well as a high decay rate. After dealing with both of these domains, all those areas which have been defined as potential aliasing areas are excluded from the extrapolation and processed separately, and as in our case, are padded with zero values in the unavailable scale which needs to be predicted.

To make the whole algorithm more robust for all kinds of images, the predicted coefficients are classified into bounded and unbounded variations [37] [38] based on the decay rate we discussed before which helps to create a precise output. As for bounded variation in the literature [37], we may defined it as areas with a set of bounded oscillations normalized over [0, 1], as expressed in equation 9.

$$\|f\|_{TV} = \int \left|f'(x)\right| dx < +\infty \tag{9}$$

Those features with variations that are infinitely divisible, or to say with independent increments among them and constitute marginal distribution, are defined as unbounded areas [38]. This classification is helpful by the enforcement of constraints on the solution space of the predicted coefficients.

In our case, after analysis of the parents' coefficients compared to the predicted ones, those which belong to bounded variations are refined by constraining the generated HR image feature, thus, information such as edge strength can be conformed to the same high level features of the LR input image. Therefore, the strategy becomes a problem of non-linear optimization of the correlation between different kinds of feature expressions between the original LR source and the estimated HR output signals.

4.1.4 IDWT Implementation

In order to reconstruct the high-resolution image, an inverse calculation of the RDWT process as shown in Figure 4 (i.e. up-sampling process needed after each filter) is necessary. This means the information about the one coarse part, as well as three detail parts of the target image are needed in order to reconstruct the target HR image (figure 12 is an example). We already obtained the horizontal and vertical coefficients from the last subsection. For the diagonal part, as it normally contains much noise, and does not contribute that much, we can just use the "lazy scheme" mentioned in [39]. For the coarse detail part, as is discussed in other papers [3] [28], it does not change much between each of the two scales. We can simply use the coarse information in scale 1 instead (i.e. the half down-sampled image of the original source as we mentioned before). Now we have all information required for image reconstruction. The sketch map of the IDWT part is shown in Figure 12.
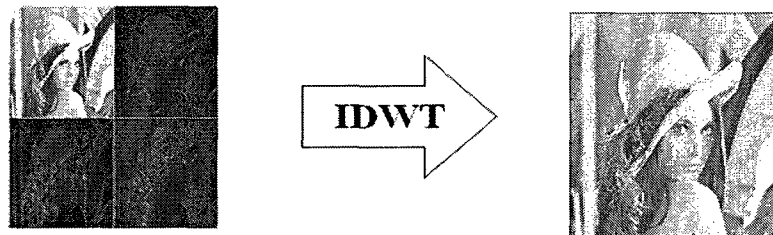

Figure 12 IDWT sketch of Lena (4×512×512→1024×1024)

From the output we find that it is not necessary to adopt the same ways to predict the vertical and horizontal information because image details differ from image to image. For example, as in the widely used Lena, there are various types of image components we have to consider. However, for Boats, there are plenty of horizontal edges we have to deal with, and for Peppers it is vertical edges instead. In order to obtain a satisfactory result, we may add weight to the horizontal part, or vertical part, or to both of them. To evaluate if the result is good or not, we can compare the result (especially edge information) with the coarse part of the input scale using MSE and use a threshold. Though the automated weight method is not well designed, we have already tried manual

ways in our proposed method, which have already shown a significant effect, and this remains a concern for future research as well.

4.2   Other Related Applications

Along with the SR system research, we have also examined a few other related research areas as well, which have significant meaning not only in the super-resolution area, but also in other image processing fields like motion detection, tracking and video surveillance etc.. The following two applications are among the major ones, and the brief theory is discussed here. The experiment results will be shown in the next chapter along with the output results. [1]

4.2.1 Foreground Extraction

Foreground pixels extraction from an image or several images is well known as an important tool commonly used in several applications of computer vision, human computer interaction, and super resolution areas. The current major techniques for direct foreground extraction require user–assistance human interaction and multiple input image sequences to generate input information. However, here we propose a novel technique that eliminates the need for user interaction. In single image input cases, the generic stochastic characterization of the salient features of an image is the main strategy of the proposed technique which provides an automatic foreground extraction performance that is competitive with existing single image methods.

As discussed in the early part of this chapter, the coefficients are classified into bounded and unbounded variations which are further classified by the decay rate of the wavelet coefficients across fine scales. By doing this we can estimate the bound of the oscillations. Furthermore, those variations which are unbounded represent the clutter, texture, and in

---

[1] All the works mentioned in 4.2 were done with the help of Mr. Michael Chukwu at University of Windsor.

some cases noise, in images. No prominent significance is contained in these kinds of features but they are usually found in most natural images. The bounded oscillations in the three sub-bands (i.e. horizontal, vertical, and diagonal) are scanned with the established proximity of the coefficients following the direction of the transformer which connect pixel points, in order to extract near rigid objects, shapes, and patterns in the image defined by these coefficients. Simple model of the discussed theory is shown in equation 10.

$$p(I(x,y)) = p(U(x,y)) + p(B(x,y))$$

(10)

where B (x, y) represents the salient features of the image, and U (x, y) is the clutter, noise and other features not prominent and hence be ignored by this approach.

The Lipschitz Exponents for each feature in the input image is computed separately, as we did in the SR process before, providing the metric for the classification. Here, pre-evaluation of the values using a hard threshold is carried out prior to the classification which is used to estimate the existence of a definite foreground or the blurriness of the input image. By doing that, the range of the values is used as a scale to classify the image features into foreground and background, with those likely factors linearly related to the magnitude for the image foreground.

4.2.2 Change Detection

For the extraction and detection of activities in background scenes, change detection in temporally related image sequences is a primary method. There are a vast and wide range of applications ranging from security and surveillance to fault detection and power savings in the related areas. And for the estimation and prediction of these changes, the prevalent methods for change detection are derived from the different extractions where differences in the gray-level values of the pixels between two or more consecutive images sequence are used. However, these approaches, and its derived modifications, are largely dependent and reliant on the application value of thresholds which are used to provide significance to the differences in order to compensate for the vulnerability of

these methods in illuminating variability and noise. Therefore, we propose a frequency domain approach to change detection which eliminates the need for thresholds and provides comparatively superior performance to the existing algorithms in order to deal with the existing problems.

It is the determination of the change mask across image sequence $I_{1...N}$, where $N = 2$ where the problem of change detection is modeled on. We pre-suppose in the proposed change detection algorithm that the alignment of the image sequence is in the same co-ordinate system. Normally if we face an ideal scenario, the difference in the image pair can be extracted from the simple signed difference. However, the factor of noise and illumination can distort this status. Hence mechanisms for the compensation of the two factors are needed to be implemented.

To eliminate the impact of noise, we prefer to use the spectral content generated from RDWT of the image pair, in order to provide the space-frequency information. Upon the different core requirements for high spatial resolution, the choice of wavelet is predicated differently. By doing this, wavelet coefficients are influenced by the large amount of neighboring pixels. In this way, we can largely reduce the effects of noise to minimal deviations in coefficient values across the image pair. The sketch of the whole process is shown in figure 13. This is also useful in Multi-frame and video input SR algorithms.
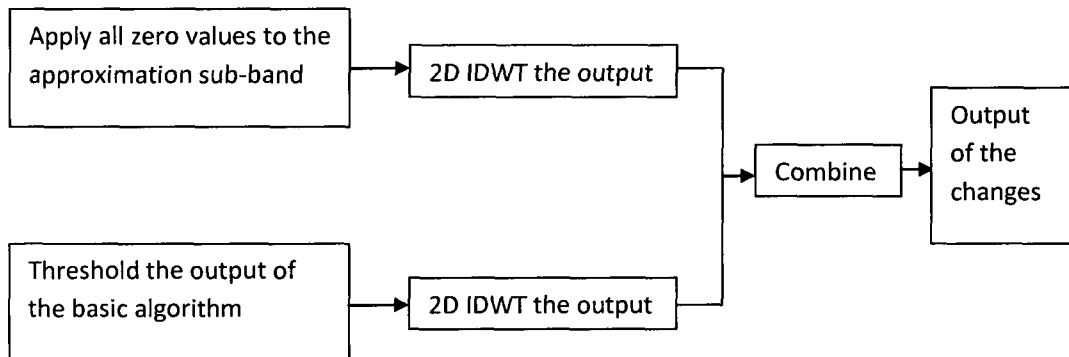

Figure 13 Two different input frames changes generation

CHAPTER 5

EXPERIMENT RESULTS AND DISCUSSION

5.1   Experimental Results of the Proposed SR Algorithm

The performance of the proposed algorithm is tested with both subjective and objective point of view. And all the algorithms are tested using Matlab. From a subjective point of view, we can focus on the effects of de-blurring, de-noising, and alias removal on the output HR image. Also, we seek differences between the original image and the output where human eyes can distinguish. Figure 14 is an example of the subjective judgment of SR outputs. bottom left one is good, while bottom right one is poor.
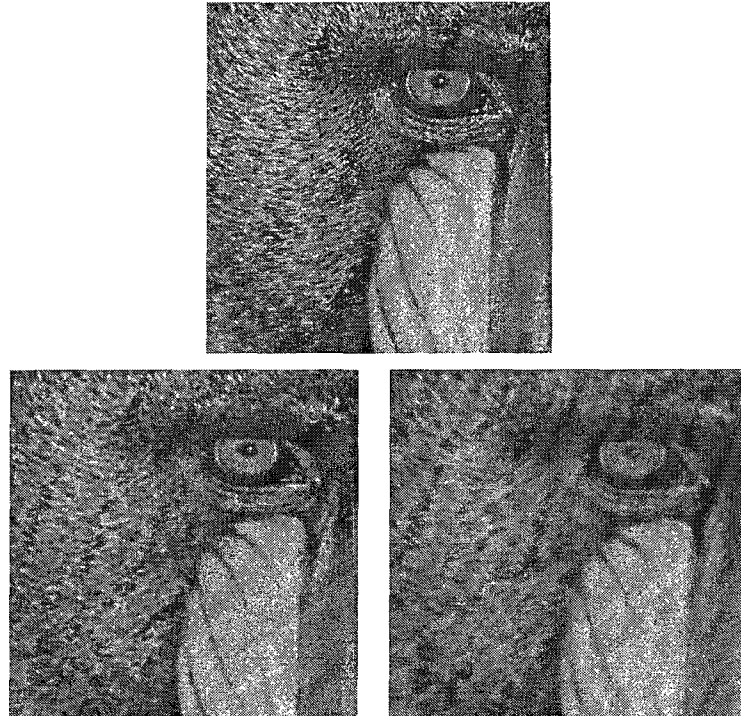
Figure 14 Example of the subjective judgment of SR outputs
(Top: original; down left: good output; down right: bad output)

From the objective point of view, PSNR is widely adopted to test interpolation algorithms. Thus, we also utilized PSNR for evaluation and comparison. Image details differ from image to image, as for example, the widely used Lena, there are various types of image components we have to consider; however, as for Boats, there are plenty of horizontal edges we have to deal with. For Peppers, it is vertical edges instead. In order to obtain a satisfactory result, we adopt the standard images like Lena (also called Lenna), Boat, Bridge, Peppers, and Barbara etc. as test images in order to ensure the stability of the whole system. The first DWT LL output is used as the input source so that we can use the original image to test the PSNR. The Daubechies's biorthogonal 9/7 filter is used in all the processes including the DWT to get the input, the RDWT and the IDWT part. This guarantee the uniqueness of the whole process and the best result in the same platform, as it was proven that Daubechies's biorthogonal 9/7 filter is one of the best filters in the interpolation algorithm [39]. Another effect we have to be aware of is Zero-padding, which is also called the "lazy" way [39], is a good standard for interpolation algorithms. We also adopt this method for comparison in our paper. The bi-cubic results are used as the compare standard in PSNR. And to highlight the improvement of our results, the results of other algorithms [20] [24] [40] are also compared as contained in the documentation using similar evaluation metrics.

In comparison with the standard zero-padding SR algorithm, we show the results of the proposed SR algorithm on eight different 8 bit grayscale images (Figure 15-22) among which different kinds of image detail information are involved. All those images, including Lena (also called Lenna), Boat, Bridge, Peppers, Barbara, Baboon, Airplane, and Elaine are widely used in image processing, especially in the SR area. The input image is up-scale from 256 X 256 to 512 X 512. The images to be shown here contain the original source image, the down-sized image, and the result from the proposed algorithm as well as the result from the zero-padding algorithm. The objective judgment follows the comparison of the PSNR values (equation 11) for the reconstructed images of higher resolution against an image sampled at that resolution without extraneous details.

$$PSNR = 20 \times \log 10(b / rms)$$

(11)

where b is the largest possible value of the signal (typically 255 or 1), and rms is the root mean square difference between the two images. The PSNR is given in decibel units (dB), which measures the ratio of the peak signal and the difference between two images.
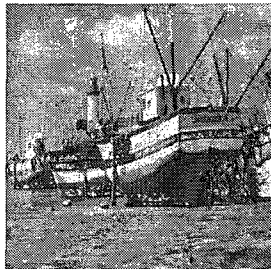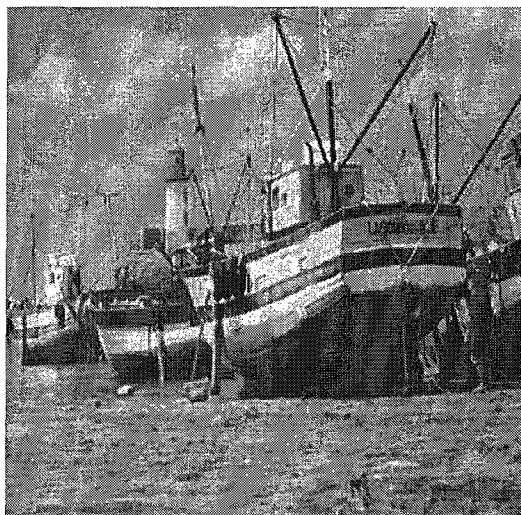

(a)

(b)

(c)

(d)

Figure 15 SR outputs using Lena as input

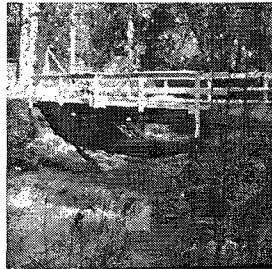**(a: original; b: down-sized image; c: proposed SR result; d: zero-padding SR result)**

31

(a)

(b)

(c)

(d)

Figure 16 SR outputs using Boat as input

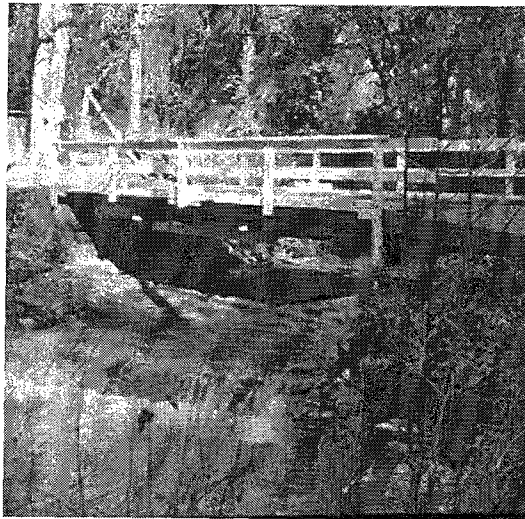**(a: original; b: down-sized image; c: proposed SR result; d: zero-padding SR result)**
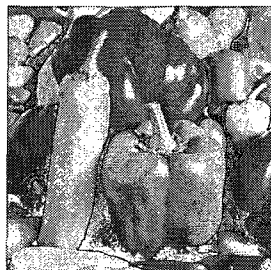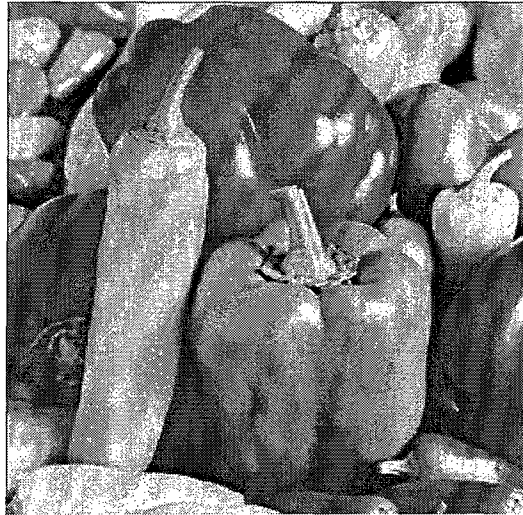
(a)

(b)

(c)

(d)

Figure 17 SR outputs using Bridge as input

(a: original; b: down-sized image; c: proposed SR result; d: zero-padding SR result)
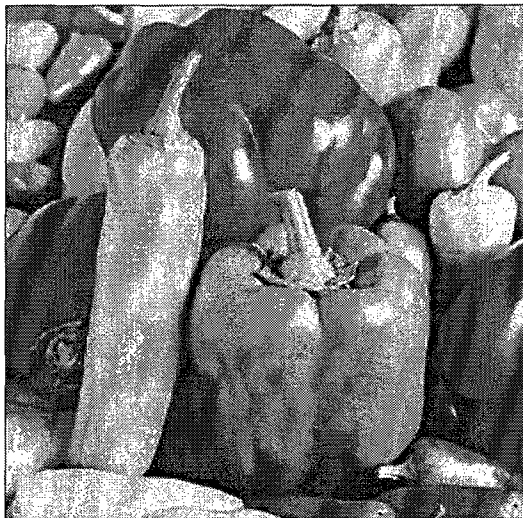
(a)

(b)

(c)

(d)

Figure 18 SR outputs using Peppers as input

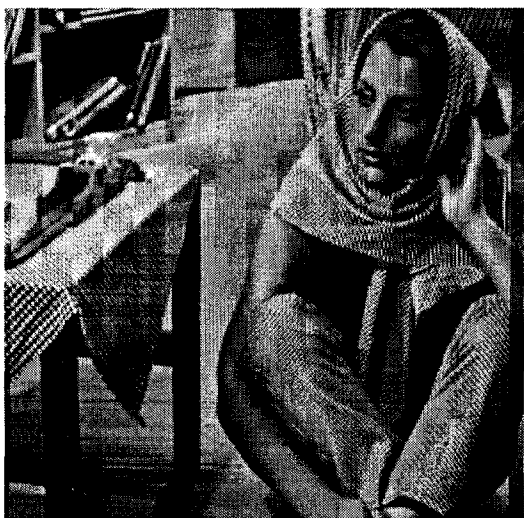**(a: original; b: down-sized image; c: proposed SR result; d: zero-padding SR result)**
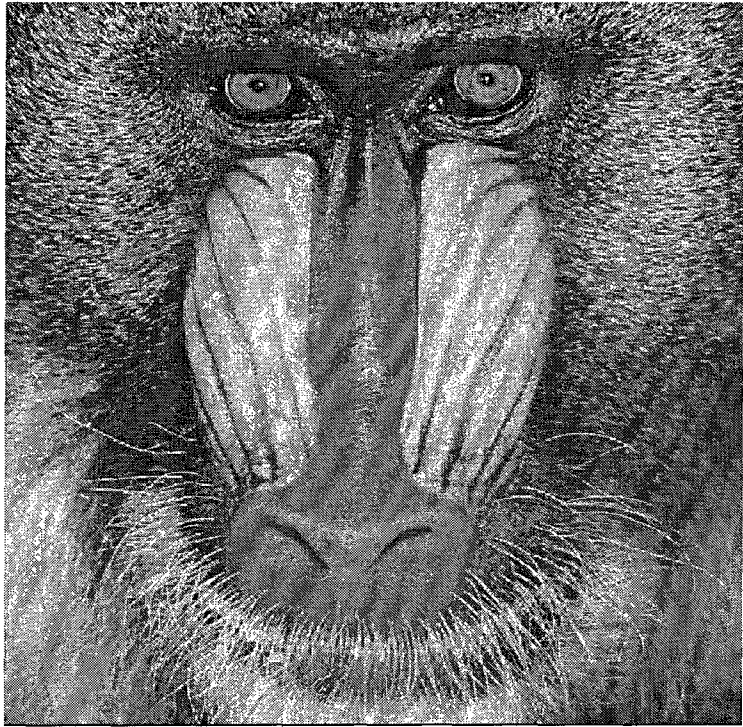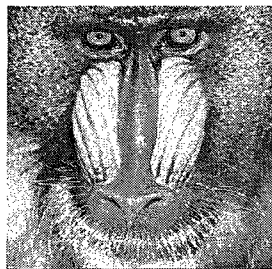
(a)

(b)

(c)

(d)

Figure 19 SR outputs using Barbara as input
(a: original; b: down-sized image; c: proposed SR result; d: zero-padding SR result)

(a)

(b)

(c)

(d)
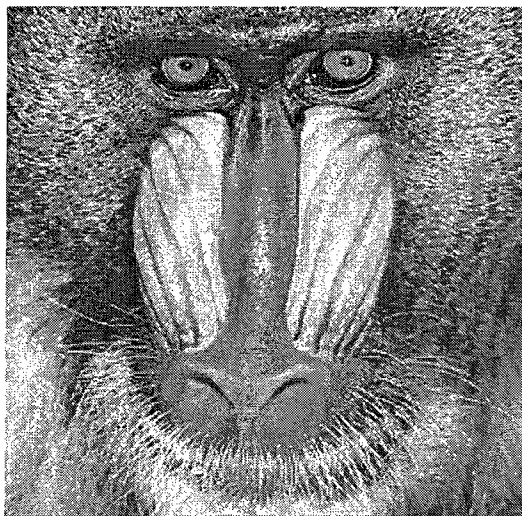
Figure 20 SR outputs using Baboon as input

(a: original; b: down-sized image; c: proposed SR result; d: zero-padding SR result)

(a)

(b)

(c)

(d)

Figure 21 SR outputs using Airplane as input

(a: original; b: down-sized image; c: proposed SR result; d: zero-padding SR result)

(a)

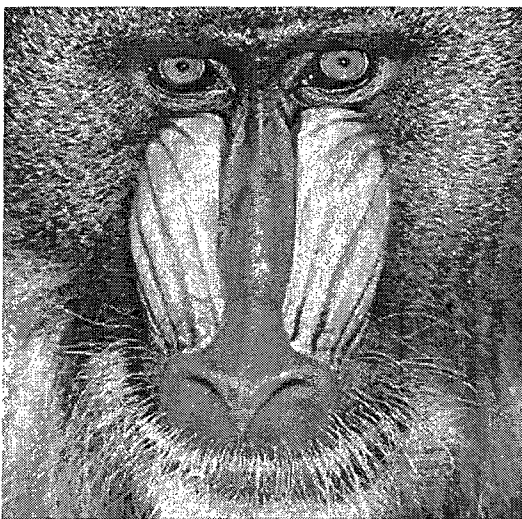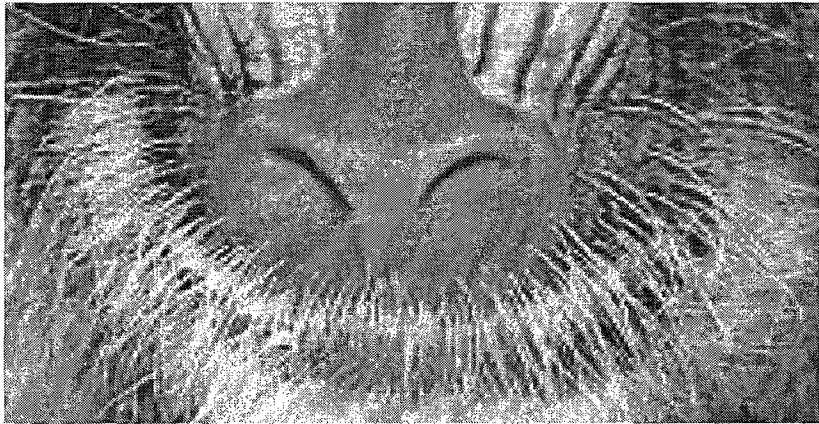**(b)**

(c)

(d)

Figure 22 SR outputs using Elaine as input
(a: original; b: down-sized image; c: proposed SR result; d: zero-padding SR result)

(a)
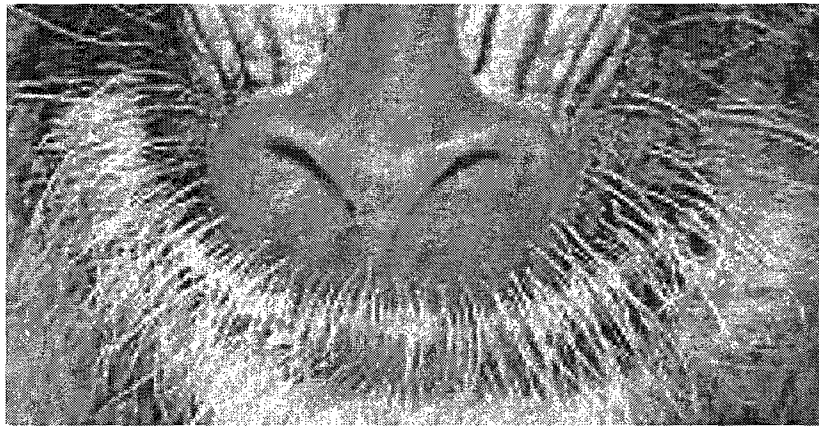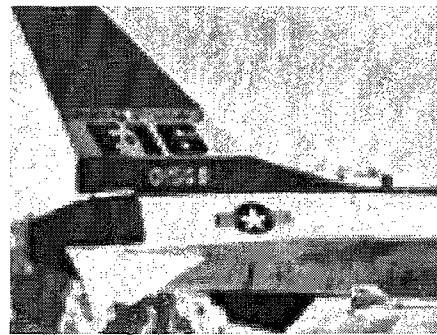

(b)

(c)

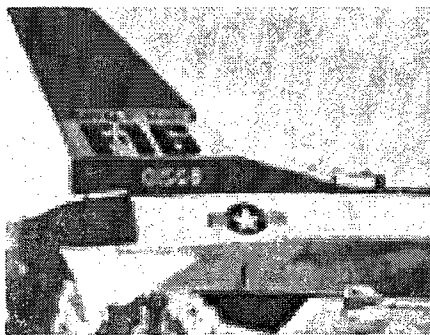**(d)**

Figure 23 Detail from Proposed and Zero-padding SR outputs

(for each group, the front one is from proposed SR, the latter is from zero-padding)

From the results of the proposed algorithm and the zero-padding algorithm as well as part of enlarged details (Figure 23) from some of the outputs, we can find an obvious improvement in the whole outputs, also in details where better performance on reserving the smooth edges can be found by the proposed algorithm. As the space is limited, those are only a very small part of our work. Plenty of images have been tested to ensure the robustness of the proposed algorithm.

To make the results more convincing, we tested all the PSNR results between the output of the proposed algorithm and the original source image, as well as those between the output of the standard method and the original source image, and put all the eight (i.e. those eight images shown above are used) PSNR comparison results in Table 2.

Table 2 Simulation PSNR Results for Proposed SR and Standard SR

(image size: 256 X 256 → 512 X 512)

PSNR (dB)	Lena	Boat	Bridge	Peppers	Barbara	Baboon	Airplane	Elaine
Proposed	34.74	29.59	25.30	26.94	24.55	23.16	27.14	26.88
Standard	32.71	28.60	24.35	26.83	24.35	22.95	26.22	25.26

From the Table 2, it can be observed that our results are better than the standard SR method (i.e. zero-padding) by one or two "dB"s which is good in traditional image processing projects. Since all the images we used are chosen randomly, and contain different kinds of edge information, obtained results are proven to be competitive and robust.

From other state-of-art research literatures, we can also find the PSNR results between their results and the standard source images. And to make our results more sophisticated, we also compare those major ones with ours as well in the following Table 3.

Table 3 Simulation PSNR Results for Proposed SR and State-of-art SR

(image size: 256 X 256→512 X 512)

PSNR(db)	Lena	Boat	Bridge	Peppers
Bi-cubic spline	30.10	26.36	24.33	26.51
Kinebuchi[20]	30.38	27.12	24.12	26.52
Tian/Ma [24]	32.87	27.40	*25.45*	26.21
Vandewalle[40]	30.21	25.97	23.21	26.89
Proposed	*34.74*	*29.59*	25.30	*26.94*

All the best results have been set in italic to make them more prominent, from which we can find clearly that, though Kinebuchi's work [20] is a little better than ours in the Bridge image, overall better results can be found in our proposed algorithm.

5.2 Experimental Results of the Proposed Foreground Extraction Algorithm

Results of one of the related applications, which is the single frame foreground extraction algorithm discussed before are shown here. The algorithm is implemented using Redundant Discrete Wavelet Transform with Cohen-Daubechies-Feauveau 9/7 wavelet filter and the multi-resolution analysis is performed. The feature extraction analysis based on the proposed method shows comparative performance across a wide range of images. As it is a side application of SR, only part of the experimental results are shown here considering several traditional images as examples of salient feature extraction, the extract of the image corresponding to the bounded oscillations is presented in Figure 24.
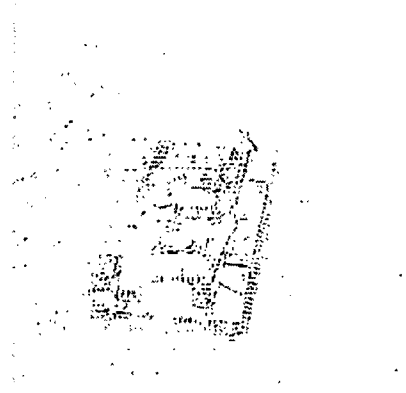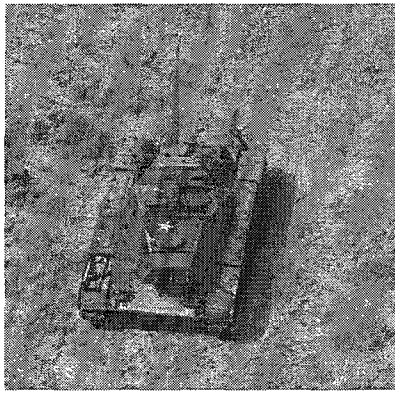
(a) Tank

(b) Armored Car

50
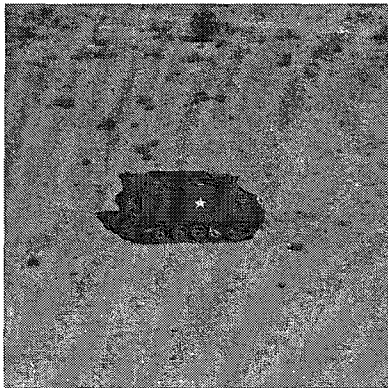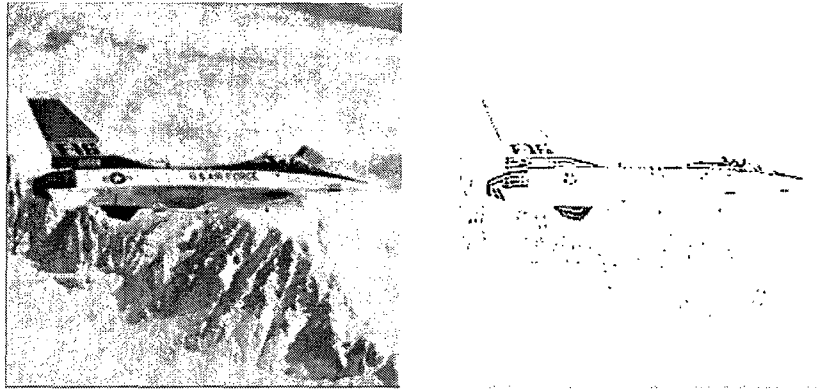
(c) Airplane

Figure 24 Results of proposed foreground extraction algorithm

(left: original images, right: outputs)

5.3 Experimental Results of the Proposed Change Detection Algorithm

Another related application discussed earlier is the change detection algorithm and is tested here. By doing this, we also hope to extend this to HD video processing in the future research. The experimental evaluation of the change detection algorithm is performed in two categories of tests, which are original input and input with noise and is presented in the following Figure 25. From those it is clear that our proposed algorithm is robust even in the noisy input environment.
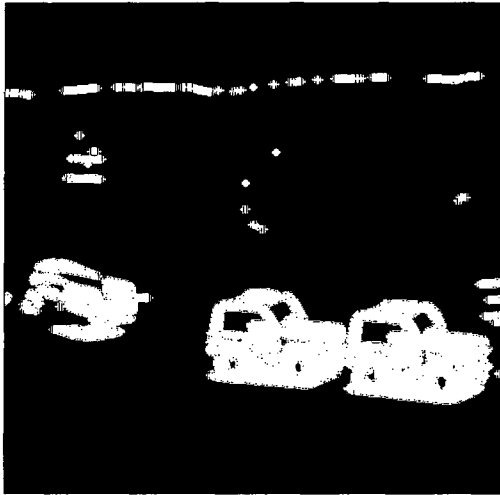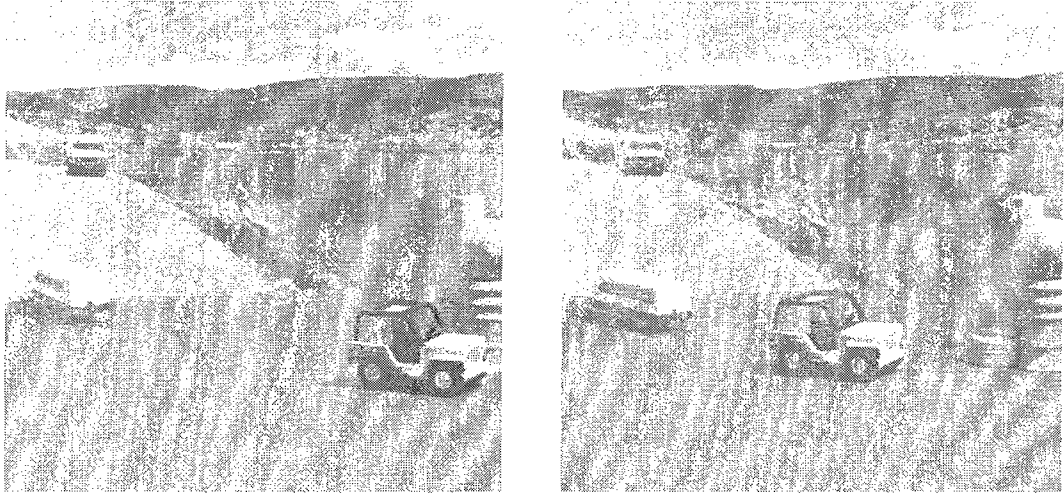
(a) Simple image scenes
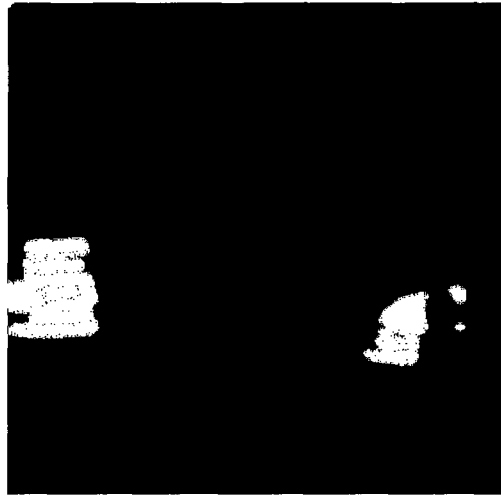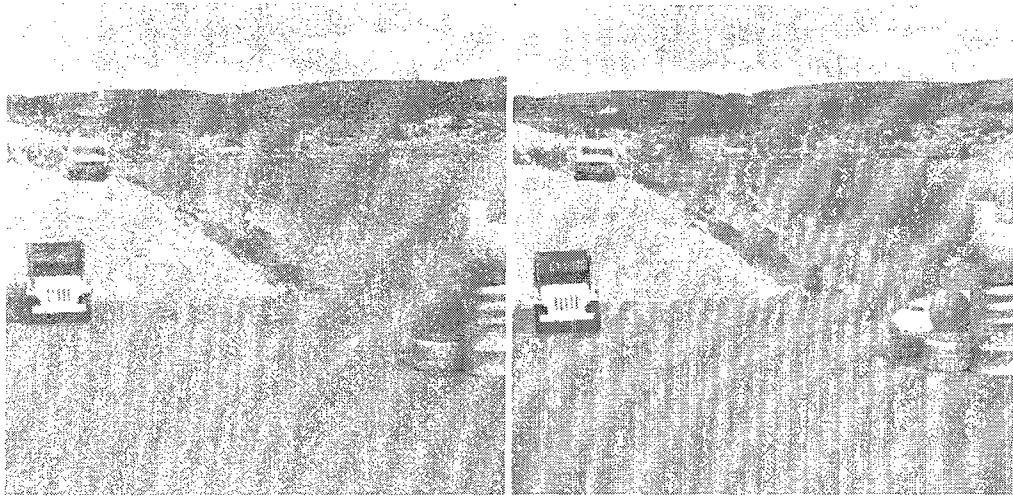
(b) Image scenes with noise

Figure 25 Results of proposed change detection algorithm
(top two: original input images, down: different outputs)

CHAPTER 6

CONCLUSIONS AND FUTURE WORK

6.1 Conclusions

In this thesis an edge-adaptive RDWT-based image interpolation algorithm is presented. Edge information, which is a sharp variation of wavelet transform in finer scales in both vertical and horizontal directions, is used to predict the high-frequencies needed to reconstruct high-resolution images. Weighted calculations for the details of high-resolution are adopted to make the algorithm more robust. The aliasing problem has been well removed by differentiating the bounded and unbounded areas in the source image. This is a good strategy which can be used in many other image processing areas as well.

For the consideration of tractility and the convenience of testing, the whole system has been divided into three modules, which are preprocessing, super-resolution and aliasing management parts. By doing this, the expansibility of the system is obvious, in time consumption, the veracity of the algorithms themselves, as well as in hardware feasibility, which is parallel processing of each module can be considered during hardware design in order to increase the possibility of real-time processing needed in real life applications.

By doing lots of testing on different kinds of single images and the analysis of the experimental results, the objective quality (PSNR) as well as the subjective quality (edge detail) have been improved, compared to the standard method (Zero-padding) and other popular state-of-art methods in literatures. This is a strong proof that the proposed super resolution algorithm provided a good ability to recover the lost high frequency information in under-sampled images in order to generate the target HR image.

6.2 Future Work

Though the output of the proposed algorithm is good, there are still several aspects which can be further explored in the future.

(1) For the SR system itself:

We are planning to modify the way to predict the detail coefficients, which may be achieved by:

> Testing other orthogonal or biorthogonal wavelet filters instead of CDF 9/7.

> Testing other methods like Contourlet and Curvelet, instead of RDWT.

Also, we want to do some research on Multi-inputs SR, as well as the SR used in camera networks which is a brand new area.

(2) Modify the system and develop a hardware facility to apply this to industry, with which to predigest the time consuming system by trying the following strategy:

> Do the preprocessing process and aliasing detection act synchronously.

> Separate the non-aliasing and aliasing functions using a different algorithm strategy.

(3) We want to consider other related applications such as the HD video processing discussed before.

REFERENCES

[1]   G. Park, S. C., Park, M. K., & Kang, M. G., "Super-resolution image reconstruction: A technical overview," IEEE Signal Processing Magazine, Special issue of Super-Resolution Image Reconstruction, 20(3), pp. 21–36, 2003.

[2]   J.D. van Ouwerkerk, "Image super-resolution survey", Image and Vision Computing, 24(10), pp. 1039-1052, 1st Oct., 2006.

[3]   G. Park, S. C., Park, M. K., & Kang, M. G., "Super-resolution image reconstruction: A technical overview," IEEE Signal Processing Magazine, Special issue of Super-Resolution Image Reconstruction, vol. 20, no. 3, pp. 21–36, May 2003.

[4]   Chaudhuri, S., & Joshi, M. V., "Motion-free super-resolution," New York: Springer, 2005.

[5]   C.V.Jiji, Subhasis Chaudhuri, Priyam Chatterjee, "Single frame image super-resolution: should we process locally or globally?," Multidim Syst. Sign Process, vol. 18, pp. 123–152, Mar. 2007.

[6]   Chaudhuri, S., "Super-Resolution Imaging," Kluwer Academic Publisher, Boston, 2001.

[7]   Papoulis, A., "A new algorithm in spectral analysis and band-limited extrapolation," IEEE Transactions on Circuits and Systems, CAS-22(9), pp. 735–742, 1975.

[8]   Harris, J. L., "Diffraction and resolving power," Journal of Optical Society America, 54, pp. 931–936, 1964.

[9]   Jiji, C. V., & Chaudhuri, S., "PCA based generalized interpolation for image super-resolution," In Proceedings of the Indian conference on computer vision graphics and image processing, pp. 139–144, 2004.

[10]   C.B. Atkins, C.A. Bouman, J.P. Allebach, "Optimal image scaling using pixel classification," Proceedings of International Conference on Image Processing, pp. 864–867, 2001.

[11]   C. Staelin, D. Greig, M. Fischer, R. Maurer, "Neural network image scaling using spatial errors", HP Laboratories Israel, Oct. 2003.

[12]   F.M. Candocia, J.C. Principe, "Superresolution of images based on local correlations", IEEE Transactions on Neural Networks 10 (2), pp. 372–380,1999.

[13]   M.F. Tappen, B.C. Russell, W.T. Freeman, "Exploiting the Sparse Derivative Prior for Super-Resolution and Image Demosaicing, " 2003.

[14]   M.J. Black, G. Sapiro, D.H. Marimont, D. Heeger, "Robust anisotropic diffusion," IEEE Transactions on Image Processing 7 (3) , pp. 421–432, 1998.

[15]   S. Battiato, G. Gallo, F. Stanco, "Smart interpolation by anisotropic diffusion," Proceedings of 12th International Conference on Image Analysis and Processing, pp. 572–577, 2003.

[16]   X. Li, M.T. Orchard, "New edge-directed interpolation," IEEE Transactions on Image Processing 10 (10), 1521–1527, 2001.

[17]   S. Battiato, G. Gallo, F. Stanco, "A locally-adaptive zooming algorithm for digital images," Image Vision and Computing Journal 20 (11), pp. 805–812, 2002.

[18]   Parker, J. Anthony, Kenyon, Robert V. Troxel, Donald E. "Comparison of Interpolating Methods for Image Resampling" IEEE Transactions on Medical Imaging, Volume: 2, Issue: 1, pp. 31-39, Davis, CA, USA, March 1983.

[19]   Emil DUMIC, "The use of wavelets in Image Interpolation: Possibilities and limitations," Radioengineering, Volume 16, No. 4, pp 101-109, December 2007.

[20]   Kinebuchi, K. Muresan, D.D.   Parks, T.W., "Image interpolation using wavelet based hidden Markov trees", IEEE International Conference on Acoustics, Speech, and Signal Processing, Volume: 3, pp. 1957-1960, Salt Lake City, UT, USA, 2001.

[21]   Dong Him Woo,   Il Kyn Eom,   Yoo Shin Kim, "Image Interpolation based on inter-scale dependency in wavelet domain" International Conference on Image Processing, Volume: 3, pp. 1687- 1690, 2004.

[22]   Vladan Velisavljevic, "Edge-preservation resolution enhancement with oriented wavelets", Proceedings of the International Conference on Image Processing, ICIP 2008, October 12-15, 2008, San Diego, California, USA. IEEE 2008.

[23]   Yu-Len Huang, Ruey-Feng Chang, "MLP interpolation for digital image processing using wavelet transform," IEEE International Conference on Acoustics, Speech, and Signal Processing,15-19, Volume: 6, pp. 3217-3220, Phoenix, AZ, USA, Mar 1999.

[24]   Jing Tian and Kai-Kuang Ma, "Edge-Adaptive Super-Resolution Image Reconstruction Using A Markov Chain Monte Carlo Approach" 6th International Conference on Information, Communications & Signal Processing, 10-13 pp. 1-5, Singapore, Dec. 2007.

[25]   Y. Meyer, "Ondelettes et Operateurs," New York: Hermann, 1990.

[26]   S. Mallat and W. L. Hwang, "Singularity detection and processing with wavelets," IEEE Trans. Inform. Theory, vol. 38, no. 2, pp. 617–643, Mar. 1992.

[27]   S. Mallat and S. Zhong, "Characterization of signals from multiscale edges," IEEE Trans. Pattern Anal. Machine Intell., vol. 14, no. 7, pp. 2207–2232, Jul. 1992

[28]   S. G. Chang, Z. Cvetkovic´, and M. Vetterli, "Resolution enhancement of images using wavelet transform extrema extrapolation," in Proc. IEEE Int. Conf. Acoust., Speech, Signal Processing, vol. 4, pp. 2379–2382, May 1995.

[29]   S. Grace Chang, ZoranCvetković, "Locally Adaptive Wavelet-Based Image Interpolation," IEEE Trans. Image Process, vol. 15, no. 6, pp. 1471-1485, 2006.

[30]   Do,M. N. "Directional multiresolution image representations," PhD thesis. Lausanne, Switzerland: Swiss Federal Institute of Technology, 2001.

[31]   Do, M. N., & Vetterli, M. "The contourlet transform: An efficient directional multiresolution image representation," IEEE Transactions on Image Processing, 14(12), pp. 2091–2106, 2005.

[32]   Roweis, S. T., & Saul, L. K., "Nonlinear dimensionality reduction by locally linear embedding". Science, 290, pp. 2323–2326, 2000.

[33]   Xin Li, "Edge directed statistical inference and its applications to image processing," PhD thesis in Princeton University, Nov. 2000.

[34]   J. F. Canny, "A computational approach to edge detection," IEEE Trans. Pattern Anal. Mach. Intell., vol. 8, no. 6, pp. 679–698, Nov. 1986.

[35] Deqiang Li, Haibo Luo, Zelin Shi, "Redundant DWT Based Translation Invariant Wavelet Feature Extraction for Face Recognition," 19th International Conference on Pattern Recognition, pp. 1-4, 2008.

[36] I. Daubechies: Ten Lectures on wavelets, SIAM, 1992.

[37] Mumford D., and Gidas B., "Stochastic Models for Generic Images", Quarterly of Applied Mathematics, volume LIV, issue 1, pp. 85-111, March 2001.

[38] Cohen, A., Devore, R., Petrushev, P., and Xu, H., "Nonlinear approximation and the space", BV(R2)., Amer. J. Math., 121, pp 587-628, 1999.

[39] Xin Li, "Image Resolution Enhancement via Data-Driven Parametric Models in the Wavelet Space," EURASIP Journal. on Image and Video Processing, vol. 2007, issue 1, pp. 1-12, Jan. 2007.

[40] Patrick Vandewalle, Sabine Süsstrunk, and Martin Vetterli, "A Frequency Domain Approach to Registration of Aliased Images with Application to Super-resolution," EURASIP Journal on Applied Signal Processing, vol. 2006, Article ID 71459, 14 pages, 2006.

VITA AUCTORIS

Fei Yu was born in 25 April, 1985 in Nan Jing, Jiang Su, China. He obtained his B.A.Sc. in Electronic Engineering and Optoelectronic Techniques department from Nanjing University of Science and Technology in Nan Jing, China, where he graduated in 2008.

In Fall 2008, Fei began the pursuit of a M.A.Sc. degree in Electrical Engineering under the supervision of Dr. Jonathan Wu at the University of Windsor, Windsor, Ontario, Canada. During this period, he has received University of Windsor Graduate Teaching Assistantship and Research Assistantship Scholarship. His area of specialization has been the Image Super-resolution System Design and other related image processing areas.